Total reaction cross section for protons on ^{3}He and ^{4}He between 18 and 48 MeV†

A. M. Sourkes, A. Houdayer, and W. T. H. van Oers
Department of Physics, University of Manitoba, Cyclotron Laboratory, Winnipeg, Manitoba, Canada R3T 2N2

R. F. Carlson
Department of Physics, University of Redlands, Redlands, California 92373

Ronald E. Brown
John H. Williams Laboratory of Nuclear Physics, University of Minnesota, Minneapolis, Minnesota 55455

(Received 25 August 1975)

An attenuation technique has been used to measure the total reaction cross section σ_R for the systems $p + {}^3$He and $p + {}^4$He at 10 and 16 incident proton energies, respectively, between 18 and 48 MeV. The attenuations were measured to about 2% and the elastic corrections are known to about 2%. This results in the σ_R values being determined to about 8%, with smaller errors than this at the high energies and larger errors than this at the low energies. The data are compared with results from elastic scattering analyses using phase shifts, the optical model, and the resonating-group method.

[NUCLEAR REACTIONS $p + {}^{3,4}$He, E_p=18–48 MeV; measured σ_R; anticoincidence beam-attenuation technique.]

I. INTRODUCTION

One of the basic measurements of importance for the understanding of the interaction between two nuclei is that of the total reaction cross section σ_R. For example, absorption processes affect the elastic scattering probability by removing flux from that otherwise available for scattering, and therefore measured values for σ_R are necessary to allow the proper restrictions to be placed on the amount of absorption included in theoretical or phenomenological analyses of elastic scattering data. Phase-shift extraction and optical-model fitting are types of such analyses. The inclusion of phenomenological imaginary potentials in resonating-group calculations[1] for light systems has also made it important to have σ_R measurements for these systems. Some such work is in progress[2-4] for the light systems ^{3}He + ^{4}He (Ref. 2), $d+d$ (Ref. 3), and ^{3}He + ^{3}He (Ref. 4) in which σ_R values are determined by summing appropriate partial reaction cross sections. In the present work we report measurements of σ_R for the systems $p + {}^3$He and $p + {}^4$He over the proton energy range 18 to 48 MeV (lab). An anticoincidence beam-attenuation technique[5-10] was used in these measurements; a brief report of the experimental results has been given.[11]

The methods used in performing the experiment and in reducing the data to total reaction cross sections are discussed in Secs. II and III. Comparisons of the present data with results from other experimental work, from optical-model calculations, and from phase-shift analyses are presented in Sec. IV. In Sec. V a discussion is given of the relevance of the present measurements to resonating-group calculations, and in Sec. VI concluding remarks are made.

II. EXPERIMENT

A. Apparatus

The University of Manitoba 50-MeV cyclotron was used to provide proton beams of the desired energies. The beam was momentum analyzed by a bending magnet and was tightly collimated before entering the total-reaction-cross-section apparatus. The magnetic field of the bending magnet was measured with an NMR probe whose resonant frequency was calibrated in terms of proton energy by measuring a series of proton energies with a differential absorption technique.[12] The technique consists in degrading the proton energy with accurately lapped Si absorbers and determining the residual proton energy through comparison with the known energies of α particles emitted by ^{241}Am and ThC. The incident proton energies are then determined from Si range-energy tables.[13] By this method the beam energy was determined to ± 100 keV. The beam energy spread after momentum analysis and collimation was about 150 keV full width at half maximum (FWHM).

A schematic diagram of the total-reaction-cross-section apparatus is shown in Fig. 1. De-

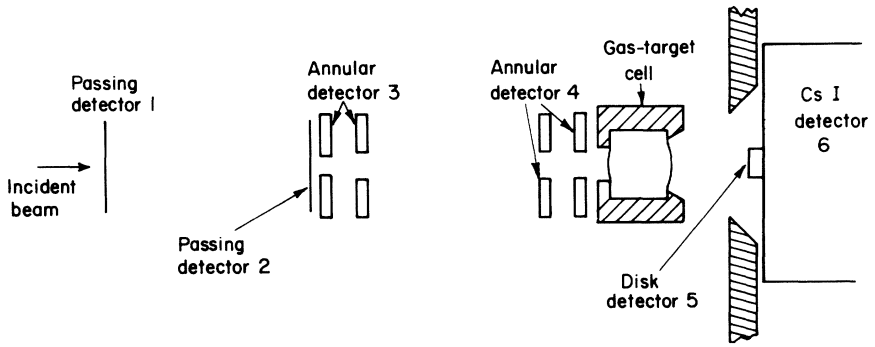

FIG. 1. Schematic diagram of the total-reaction-cross-section apparatus. Detectors 1, 2, 3, and 4 determine whether or not a proton was incident on the entrance foil of the gas-target cell, and detectors 5 and 6 help determine whether or not that proton underwent a reaction in the cell.

tectors 1 to 5 are NE-102 plastic scintillators, and detector 6 is a CsI(Na) scintillator. A trigger signal, denoted $(12\bar{3}\bar{4})$, is generated whenever detector 1 produces a signal which is in coincidence with one produced by detector 2, and at the same time, no signal is produced by either of the annular detectors 3 or 4. The presence of such an event signifies that a proton was incident on the gas-cell entrance foil. We will refer to protons producing such $(12\bar{3}\bar{4})$ events as "incident protons" and will denote the number of such events by I_0. Particles emerging from the gas cell in the forward cone enter the detector assembly composed of the thin small-diameter plastic disk 5 and the stopping detector 6. The discriminator settings are such that detector 5 is sensitive to essentially all the charged particles which enter it, and detector 6 is sensitive only to the elastically scattered protons which enter it. A signal, denoted $(5+6)$, which is generated by the occurrence of signals from detector 5, or detector 6, or both, is recorded as a "nonattenuation" event. The number I of such nonattenuation events, when combined with appropriate corrections, helps to determine how many of the number I_0 of incident protons underwent reactions in the gas cell. This manner of operation of detector 5 allows a great reduction in the correction which need be applied for reactions which occur in stopping detector 6. A detailed description of the reaction apparatus and electronic circuitry is given in Ref. 10.

The gas-target cells have walls formed by a thick brass cylinder and each cell has a beam-entrance and a beam-exit foil soldered in place and composed of Ni. The entrance foils are 0.02-mm thick and the exit foils, having a larger area than the entrance foils, are 0.07-mm thick. Two cells of different lengths were used during the experiments. One cell of length[14] $t=3.10$ cm was operated at a pressure of about 35 atm, and the other of length $t=5.16$ cm was operated at a pressure of about 20 atm. The helium gas pressure P was measured with an accurately calibrated Bourdon gauge, and the temperature T was determined with a precision thermistor in contact with the cell. The accuracy with which P, T, and the cell length t were determined results in nt, the number of helium nuclei per cm^2 in the target, being known to better than $\pm 0.5\%$.

B. Procedure

The experiment was carried out by making two separate attenuation measurements at every beam energy, one with the gas cell filled with helium and the other with the gas cell evacuated. In order to gain some knowledge about the reproducibility of the data, each of these two measurements was made as a sequence of three, with 10^7 incident protons being recorded for each measurement of the sequence. The measurements made with the evacuated cell are necessary to correct the measurements made with the filled cell for the reactions and large-angle scatterings which occur in the cell foils. Therefore, the measurements at each energy yield directly an uncorrected reaction cross section σ_{un} given by

$$\sigma_{un}=\frac{1}{nt}\left(\frac{I_0-I}{I_0}-\frac{i_0-i}{i_0}\right), \tag{1}$$

where I_0 and I are the numbers of incident protons and nonattenuation events, respectively, for the filled-cell measurements, i_0 and i are the corresponding quantities for the evacuated-cell measurements, n is the number of helium[15] nuclei per cm^3 in the filled cell, and t is the length of the gas cell. To obtain the total reaction cross section σ_R, the quantity σ_{un} must be corrected for the fol-

lowing processes: (i) elastic scattering events counted as attenuation events, (ii) reaction products detected as nonattenuation events, (iii) elastically recoiling helium nuclei detected as nonattenuation events, (iv) nuclear reactions occurring in stopping detector 6, and (v) other small corrections, some of which result from the fact that the energy of protons emerging from the gas cell is several hundred keV higher when the cell is evacuated than when it is filled.

III. DATA REDUCTION

A. Corrections

1. Elastic scattering

Some of the incident protons will be elastically scattered by the helium to angles large enough so that nonattenuation signals (5 + 6) will not be produced. Such processes contribute to the number $I_0 - I$ of attenuation events in Eq. (1), and, because these events are not true reactions, corrections for them must be subtracted from the σ_{un} values. These corrections are by far the largest ones applied to σ_{un}, and therefore uncertainties in them contribute significantly to the final errors in σ_R. The corrections are calculated by integration of the elastic differential cross sections over the angular range for which (5 + 6) signals are not produced. This angular range depends on the point in the gas cell at which the scattering occurs, and therefore an average over the length of the gas cell must also be calculated. The cross sections for $p + {}^3$He scattering were obtained from Ref. 16, and those for $p + {}^4$He scattering were obtained from Refs. 17–21. A polynomial interpolation in energy of the calculated elastic corrections was carried out in order to obtain the final corrections listed in column 3 of Tables I and II. It is estimated that these corrections are known to ± 2%.

2. Reaction products

Reaction products which enter the disk detector 5 are recorded as nonattenuation events, and therefore corrections for these events must be added to σ_{un}. No such events are recorded by the stopping detector 6, because its discriminator is set high enough to reject reaction products from proton bombardment of helium. The corrections are calculated by appropriate integrations using the information from Refs. 22–24 for $p + {}^3$He and Refs. 17, 19, 22, and 25–28 for $p + {}^4$He. Extrapolations of differential cross sections to small angles and interpolations in energy are necessary in obtaining these corrections. They are listed in column 4 of Tables I and II, and their small values are due to the small solid angle subtended by detector 5. The error associated with these corrections is taken as ± 25% or ± 0.5 mb, whichever is larger.

3. Helium recoils

At the higher beam energies it is possible for helium nuclei which recoil from backwardly scattered protons to penetrate through the gas cell and to enter disk detector 5. Such events are recorded as nonattenuation events, and one might think this is proper because they correspond to elastic scatterings of the incident protons. However, in the calculation of the elastic corrections described in Sec. III A 1, it was assumed that such events are not detected. Therefore, corrections for recoil detection must be added to σ_{un}. These corrections are calculated by appropriate integrations of the elastic differential cross sections

TABLE I. $p + {}^3$He cross sections in mb at proton lab energies E_p in MeV. Listed are values for the uncorrected cross sections σ_{un} of Eq. (1), for the corrections to σ_{un} with their associated signs given in parentheses, and for the resulting total reaction cross sections σ_R with their standard deviations. The standard deviation in σ_{un} and in the elastic corrections is 2%.

E_p	σ_{un}	Elastic (−)	Reaction Products (+)	Recoils (+)	Reactions in 6 (−)	Light guide (−)	Exit foil (−)	σ_R
18.25	476	444	2.0	···	0.8	···	1.0	32 ± 13
19.55	442	398	2.0	···	1.0	···	1.0	44 ± 12
22.55	380	308	3.0	···	1.0	···	1.0	73 ± 10
25.05	416	321	4.0	0.4	1.0	3.0	1.0	94 ± 11
27.55	314	212	5.0	0.4	4.0	···	0.9	103 ± 8
30.05	295	191	6.0	0.3	4.0	···	0.8	106 ± 8
35.00	245	142	6.5	0.2	2.5	···	0.8	106 ± 6
40.00	214	103	7.0	0.2	2.5	···	0.7	115 ± 5
45.00	190	75	8.0	0.2	3.0	···	0.6	120 ± 5
47.65	185	66	8.0	0.1	3.0	···	0.5	124 ± 5

TABLE II. $p+{}^4$He cross sections in mb at proton lab energies E_p in MeV. Listed are values for the uncorrected cross sections σ_{un} of Eq. (1), for the corrections to σ_{un} with their associated signs given in parentheses, and for the resulting total reaction cross sections σ_R with their standard deviations. The standard deviation in σ_{un} and in the elastic corrections is 2%.

E_p	σ_{un}	Elastic (−)	Reaction products (+)	Recoils (+)	Reactions in 6 (−)	Light guide (−)	Exit foil (−)	σ_R
18.20	549	556	•••	•••	0.8	•••	0.9	−9± 16
19.90	514	514	•••	•••	1.0	•••	0.9	−2± 15
23.35	452	400	0.9	•••	0.8	•••	0.9	51± 12
24.00	444	389	1.0	•••	0.6	2.0	0.9	52± 12
24.45	423	363	1.1	•••	0.6	0.8	0.9	59± 11
25.70	399	341	1.3	•••	0.8	0.7	0.8	57± 11
27.00	376	319	1.4	•••	1.4	1.2	0.8	55± 10
28.00	368	303	1.5	•••	1.3	0.7	0.8	64± 10
30.20	345	272	1.7	•••	2.7	0.9	0.7	70± 9
32.25	315	241	2.1	•••	1.8	0.6	0.7	73± 8
34.10	294	213	2.4	2.5	2.2	0.6	0.7	82± 7
37.00	272	179	3.3	2.4	2.1	0.8	0.6	95± 7
39.60	253	154	6.3	2.4	1.5	0.6	0.6	105± 6
42.30	233	132	6.9	2.3	2.0	0.4	0.5	107± 6
44.70	218	115	7.6	2.1	2.8	0.6	0.5	109± 6
47.90	207	98	8.3	1.8	3.8	0.6	0.5	114± 5

and are listed in column 5 of Tables I and II. The error in these corrections is taken to be ± 25% or ± 0.2 mb, whichever is larger.

4. Reactions in the stopping detector

Protons elastically scattered into stopping detector 6 can initiate nuclear reactions with the detector material, and this can result in insufficient energy being deposited in the crystal to allow the recording of an elastic event. Corrections for such reactions must be subtracted from σ_{un}. These corrections are obtained by multiplying a reaction probability, calculated from the information in Ref. 29, by the number of protons which enter detector 6 but miss detector 5. The number of such protons was either measured directly during data accumulation or was calculated from elastic differential cross sections. The corrections so deduced are listed in column 6 of Tables I and II. The error in these corrections is ± 20% or ± 0.4 mb, whichever is larger. As was mentioned in Sec. II A, these corrections are small because of the use of disk detector 5. The probability of not detecting a proton because of a nuclear reaction occurring in detector 5 is negligible, and therefore, only the few percent of the total number of incident protons which both enter detector 6 and miss detector 5 contribute to this correction.

5. Other corrections

As discussed in Ref. 10, of the two methods used to collect the light from disk scintillator 5, the method which employs a Lucite light guide requires that corrections be subtracted from σ_{un}. These calculated corrections account for scatterings and reactions of protons in the light guide which cause them not to be recorded by detector 6. Column 7 of Tables I and II lists these corrections for the energies at which the Lucite guide was used. The error in these corrections is taken as ± 50%.

Corrections are subtracted from σ_{un} to account for the fact that the attenuation $i_0 - i$ measured with the gas cell evacuated is slightly smaller than that due to the cell foils when the gas cell is filled. This is because the proton energy at the cell exit foil is several hundred keV higher when the cell is evacuated than when it is filled. The small corrections for this effect are listed in column 8 of Tables I and II, and the associated error is ± 50%.

Each energy E_p listed in Tables I and II is the average beam energy at the center of the filled gas cell. No corrections have been applied to the cross sections for either beam energy spread (150 keV FWHM) or energy loss (250 keV at 30 MeV bombarding energy) in traversing the gas cell. Such corrections should be negligible, except possibly in the $p+{}^4$He resonance region just above the first reaction threshold at 23.02 MeV (see Sec. IV B). In addition, finite-beam-size and multiple-scattering corrections were estimated and found to be negligible over the ranges of incident energy and target thickness used.

B. Results

The uncorrected cross sections σ_{un} of Tables I and II have a 2% standard deviation associated with them. This 2% includes contributions from the error in the target thickness nt, from the statistical errors in the measured attenuations both with and without the cell filled with helium, and from the results of the tests for reproducibility. The corrections to σ_{un} and their uncertainties have been discussed in Sec. III A. The final corrected values for the total reaction cross sections σ_R are listed in Tables I and II and are plotted in Figs. 2 and 3. The standard deviations in the σ_R values were obtained by adding in quadrature the standard deviations in σ_{un} and in all the corrections.

IV. DISCUSSION

A. $p + {}^3$He

In Fig. 2 our measured values of σ_R for the $p + {}^3$He interaction are compared with the results of two other experiments. The crosses show the σ_R values of Ref. 30 for the $n + {}^3$H system, which is the charge-conjugate system to $p + {}^3$He. These values are in reasonable agreement with our measurements; however, the large uncertainties in the $n + {}^3$H results preclude a very meaningful comparison. The triangles show estimates based on the measurements of the reactions $p + {}^3\text{He} \rightarrow d + 2p$ and $p + {}^3\text{He} \rightarrow n + 3p$ reported in Ref. 22. These measurements yielded cross sections integrated over the center of mass (c.m.) angular range 0° to 90°, and therefore, an extrapolation of these results is necessary to account for the additional yield in the c.m. angular range 90° to 180°. This was accomplished as follows. The $^3\text{He}(p, d)$ differential cross sections were extrapolated into the backward hemisphere by using as a guide the shape of the $^4\text{He}(p, d)$ differential cross section measured in Ref. 28. This procedure is made plausible by the similarity of the forward-hemisphere shapes of these two cross sections as seen in Ref. 22. Approximate symmetry[31] about 90° was assumed for the differential cross section of the reaction $p + {}^3\text{He} \rightarrow n + 3p$, and therefore the cross sections of Ref. 22 for this reaction were doubled. These extrapolations yield $\sigma_R = 134 \pm 43$ mb at $E_p = 50$ MeV and $\sigma_R = 112 \pm 23$ mb at $E_p = 30$ MeV in agreement with our measurements, but again the errors are large.

An optical-model analysis with exchange terms of $p + {}^3$He elastic scattering over an energy range encompassing that of the present experiment has recently been carried out.[32] The total reaction cross sections (not shown in Fig. 2) resulting from the imaginary potentials of this analysis are not smooth functions of energy and generally are in marked disagreement with the present measurements. An 85-MeV analysis[33] with an exchange term in the real central part of the optical potential gave $\sigma_R = 140$ mb, a value which would seem to agree with a reasonable extrapolation of the present results.

B. $p + {}^4$He

The two lowest-energy measurements of the $p + {}^4$He total reaction cross section listed in Table II were made below the first reaction threshold at 23.02 MeV (the first reaction possible is $p + {}^4\text{He} \rightarrow d + {}^3\text{He}$). The fact that these two measurements are consistent with zero serves as a useful check of the experimental method. In Fig. 3 the 14 remaining σ_R measurements are compared with other experimental results. The square shows the result of Ref. 17 at $E_p = 55$ MeV, which was based on a measurement of 40 mb for the $^4\text{He}(p, d)^3\text{He}$ reaction cross section and an estimate of 50 to 80 mb for the total continuum yield. The triangle represents the result of Ref. 26 at $E_p = 53$ MeV, which was obtained by analyzing $p + {}^4$He reaction events in a helium-filled cloud chamber. Both results are in agreement with the present measurements. The crosses indicate values deduced by applying detailed balance to measurements[25,34] on the reaction $d + {}^3\text{He} \rightarrow p + {}^4\text{He}$. In order to avoid confusion in the figure, no errors are shown for these values, and in addition, the rapid rise, then fall, of

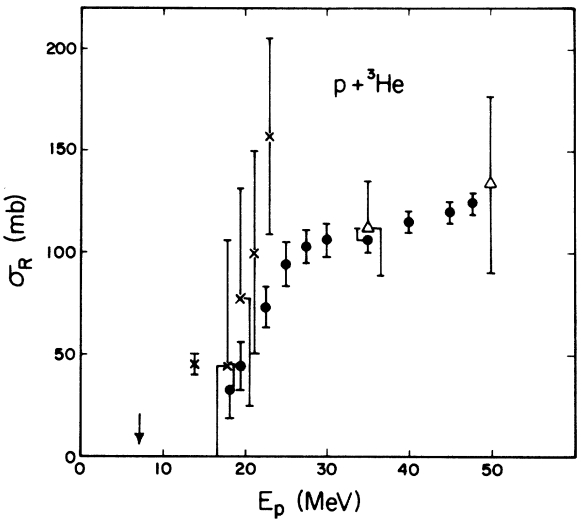

FIG. 2. Total reaction cross sections σ_R for the $p + {}^3$He interaction at proton lab energies E_p. The arrow indicates the position of the first reaction threshold. The circles represent the present measurements listed in Table I, the crosses show the measurements of Ref. 30 for the $n + {}^3$H system, and the triangles indicate values obtained from Ref. 22 by the method described in Sec. IV A.

the cross section just above threshold, which is caused by a resonance through the 16.66-MeV state[35] in ^{5}Li, is not shown. Instead, the two lowest-energy crosses show only the maximum and minimum values of the cross section across the resonance. Because the width of the ^{5}Li resonant state is less than the combined beam energy spread and target thickness, the true shape of this resonance was not observed in the present experiment. It is clear, however, that the effect of the resonance is seen in the present data through the relatively large values found for σ_R immediately above threshold. This is in contrast to the behavior of the $p+^3$He cross section shown in Fig. 2. Above 24.86 MeV additional reaction channels become open, and the crosses in Fig. 3 show increasing deviation from the present data points as the energy increases.

We also compare our measured σ_R values with those from a recent phase-shift analysis[36] of $p+^4$He elastic scattering data. In the analysis of Ref. 36, the values of σ_R given by detailed balance were used as constraints on the imaginary phases near 24 MeV. At higher energies a rough interpolation using information then available was made to obtain σ_R estimates for input to the analysis. The results for σ_R given by the final phase shifts are in excellent agreement with the present measurements. An extension[21] of the analysis to higher energies employed the present measurements of σ_R as constraints in the fitting.

In Ref. 37 an optical-model analysis was performed on $p+^4$He elastic scattering data in the energy range 30 to 55 MeV. The best-fit parameters yielded total reaction cross sections of about 150 mb, which are much too large. When σ_R was restricted to values around 95 mb, which is more reasonable in view of our measurements, the fits to the elastic data were significantly worsened. The optical-model analysis of Ref. 33, which was mentioned in Sec. IV A as having been applied to $p+^3$He scattering at 85 MeV, was also applied to $p+^4$He scattering at the same energy. In contrast to the apparent consistency between our measurements and the σ_R value obtained from the $p+^3$He analysis, the value of about 190 mb obtained from the $p+^4$He analysis seems to be too large to be reproduced by a reasonable extrapolation of the present data.

V. RESONATING-GROUP CALCULATIONS

Comparisons between results of resonating-group[38] calculations and elastic scattering data taken at energies where reaction channels are open have been facilitated by the incorporation of phenomenological imaginary potentials into the calculations. This procedure was first carried out successfully in a study[39] of the $\alpha+\alpha$ system, for which complex phase shifts over a wide energy range are available,[40] and was subsequently applied to other systems.[1,41,42] The existence of experimental values of the total reaction cross section σ_R is important in such analyses because, when there is a requirement that σ_R be fitted, there is less freedom for adjustments in the imaginary potential and therefore less chance that these adjustments can compensate for defects in the real cluster-cluster interaction obtained from the nucleon-nucleon potential through the resonating-group procedure.

Resonating-group calculations have been performed for the $p+^3$He system[43] without the inclusion of an imaginary potential. The present experimental results should prove quite useful in extending the calculations of Ref. 43 to include such a potential. In fact, the present σ_R measurements for the $p+^3$He interaction have been used to help define the imaginary potential employed in a resonating-group calculation for the $n+^3$H system.[44]

The introduction of an imaginary potential into the resonating-group treatment of the $p+^4$He system[42] proved particularly interesting because there were indications of the need for a space-exchange component in the imaginary potential. The back-angle differential cross sections and polarizations could be fitted better when such a component was included. In addition, the $p+^4$He imaginary potential used in Ref. 42 had a pure surface form

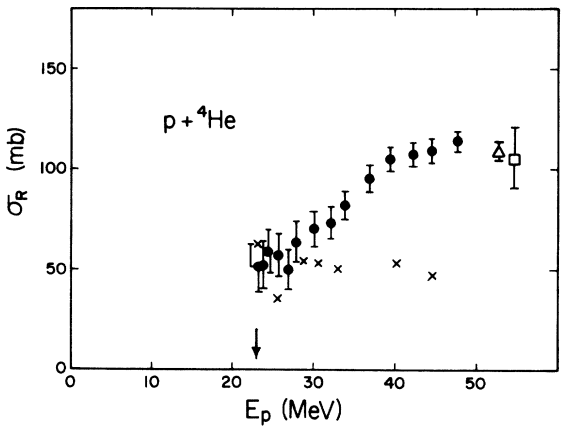

FIG. 3. Total reaction cross sections σ_R for the $p+^4$He interaction at proton lab energies E_p. The arrow indicates the position of the first reaction threshold. The circles represent the present measurements listed in Table II, the square and triangle show results from Refs. 17 and 26, respectively, and the crosses represent values deduced by applying detailed balance to measurements (Refs. 25 and 34) on the reaction $d+^3\mathrm{He}\rightarrow p+^4$He.

(Woods-Saxon derivative) with a rather small diffuseness and a rather large radius. Such a form was also inferred from an optical-model analysis[37]; however, it is in contrast to the form which has equal contributions from a volume component and a surface component and which was used in resonating-group studies of other systems.[1,39,41] On comparing our measured σ_R values with those resulting from this resonating-group calculation, we find that the calculated values are generally 30 to 40% smaller than the experimental values. We have therefore redone the analysis of Ref. 42 to learn whether or not reasonable fits to the elastic scattering data[17-19,45-47] can be obtained when the imaginary potential is required to produce σ_R values consistent with the present measurements. Although it was found possible to obtain such fits with pure surface absorption, it nevertheless was decided to perform calculations with the form originally used[39] for the imaginary potential. This was done, because, *a priori*, there seems to be no reason why the form of the imaginary potential for the $p+^4$He system should be so different from that for other systems, and therefore, it is possible that the pure surface form arises only from a compensation by the imaginary potential for defects present in the real interaction.

The formulation of the calculation follows that of Ref. 42 in which an imaginary potential iW is introduced into the integrodifferential equation derived for $p+^4$He scattering with the resonating-group method. The quantity W is given the form

$$W=(1+C_I P^r)U(r), \tag{2}$$

where

$$U(r)=-U_0\left\{\frac{1}{1+e^{(r-R)/a}}+\frac{4e^{(r-R)/a}}{[1+e^{(r-R)/a}]^2}\right\}. \tag{3}$$

In Eq. (2) P^r is a space-exchange operator, and the parameter C_I determines the strength of the exchange part of W relative to the nonexchange part. The term $C_I P^r$ introduces a $(-1)^l$ dependence into the absorptive potential. In Eq. (3) we have replaced the two strength parameters U_V and U_S of Ref. 42 by a common strength U_0. The analysis is performed by solving Eq. (1) of Ref. 42 at six energies in the c.m. energy range 23 to 44 MeV.[48] The radius R and diffuseness a of Eq. (3) are set at $R=2.25$ fm and $a=0.5$ fm, and visual fitting to the data, including the present σ_R values, is carried out by varying the two parameters U_0 and C_I. In Table III are listed the resultant values of U_0 and C_I along with the calculated total reaction cross sections σ_R, which were restricted in the fitting to agree with the present measurements. The C_I values of Table III are the same as those of Ref. 42, and here also these values result in improved fits to the elastic data at large angles. No uncertainties in C_I are indicated in Table III; however, they are very similar to those shown in Fig. 7 of Ref. 42 (± 0.1, at best). The predominence in Table III of negative values for C_I indicates that the $p+^4$He imaginary potential is generally stronger in odd orbital angular momentum states than in even. The only positive value in the table has a large uncertainty of ± 0.4.

In Fig. 4 some of the results of the calculation are compared with experimental data. In general the fits are similar to those of Ref. 42, although they are sometimes slightly worse. The most striking feature of Fig. 4 is the indication of a worsening of the fit to the polarization as the energy increases. This was also observed in Ref. 42, and is probably caused by the use of a nucleon-nucleon spin-orbit interaction rather than a tensor interaction in the resonating-group calculation. The range and depth of this spin-orbit potential were chosen to reproduce noncentral features (splitting of the p-wave phase shifts) in the $p+^4$He system at low energies. Such noncentral features are actually caused principally by the tensor interaction, and therefore, it is not surprising that a spin-orbit potential selected to reproduce such features over a restricted energy range may not be correct over a broad energy range.

The real parts of the phase shifts from the present calculation have values very close to those listed in Table II of Ref. 42. The differences are at most 0.4° and are usually much less. The most significant difference between the real parts of the phase shifts obtained from the resonating-group calculation and those obtained from the phase-shift analysis of Ref. 36 is that the calculated splitting of the d-wave phases is about twice as large as found from the phase-shift analysis. Of course, the discussion in the preceding paragraph concerning the method of including noncentral forces in the calculation is relevant to the understanding of this difference. The imaginary parts of the phase shifts from the present calculation

TABLE III. Parameters U_0 and C_I of the imaginary potential and calculated total reaction cross sections σ_R from a resonating-group analysis of the $p+^4$He system at c.m. energies E. The imaginary potential is given by Eqs. (2) and (3) with $R=2.25$ fm and $a=0.5$ fm.

E (MeV)	U_0 (MeV)	C_I	σ_R (mb)
23.04	0.75	+0.20	60.7
24.8	0.95	−0.25	70.3
32.0	1.75	−0.70	102.8
36.8	2.0	−0.70	110.8
38.2	2.1	−0.70	114.1
44.0	2.2	−0.55	117.5

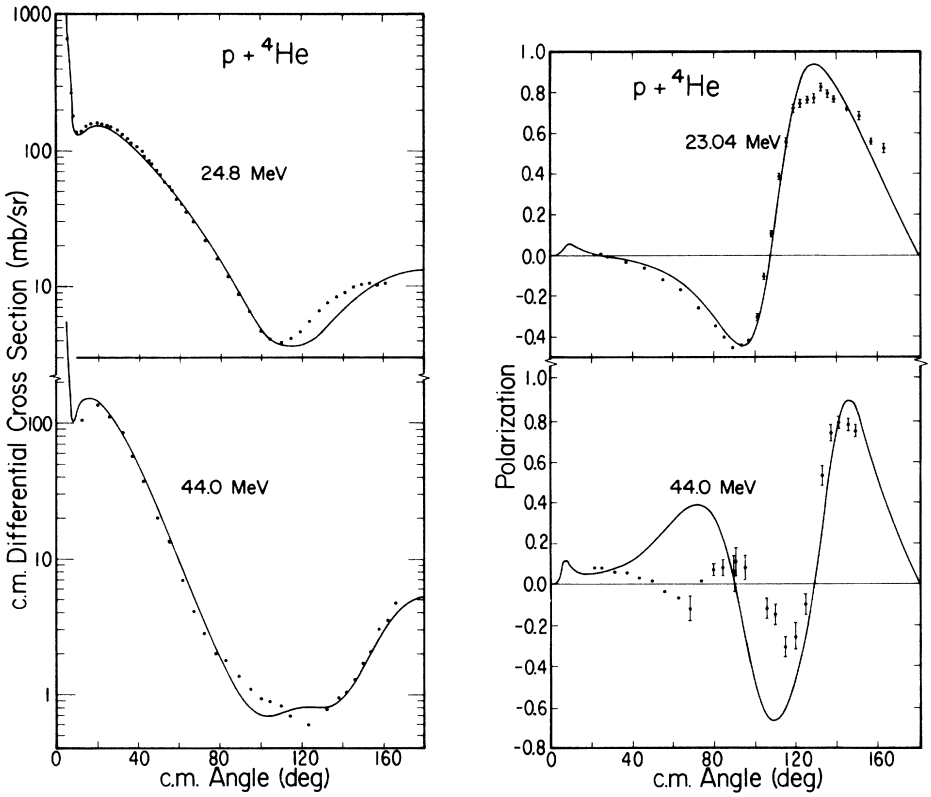

FIG. 4. Comparison of the $p + {}^4\mathrm{He}$ resonating-group calculations (curves) with the experimental data (points) of Refs. 17, 19, 45, and 47. The parameters of the imaginary potential are given in Table III.

differ from those listed in Table II of Ref. 42 principally for $l=0$ and $l=1$. The present s-wave imaginary parts are 1° to 2° larger than those of Ref. 42, and the present p-wave imaginary parts are up to 7° larger than those of Ref. 42. The most striking difference between the imaginary parts of the phase shifts obtained from the present calculation and those obtained from the phase-shift analysis of Ref. 36 is that the calculated imaginary parts are largest for $l=1$, whereas the phase-shift analysis yielded the largest imaginary parts for $l=2$.

VI. CONCLUSION

We have here reported on measurements of $p + {}^3\mathrm{He}$ and $p + {}^4\mathrm{He}$ total reaction cross sections σ_R over the proton lab energy range 18 to 48 MeV. These are the first such measurements carried out on these systems in which an anticoincidence beam-attenuation technique[5-10] was used. In the energy range 23.02 to 24.86 MeV, where the only possible reaction is $p + {}^4\mathrm{He} \rightarrow d + {}^3\mathrm{He}$, our $p + {}^4\mathrm{He}$ σ_R measurements agree with values deduced by applying detailed balance to measurements[25,34] on the reaction $d + {}^3\mathrm{He} \rightarrow p + {}^4\mathrm{He}$. In addition, values of σ_R extracted from other experiments[17,22,26,30] agree with ours, but the uncertainties in these other values are large. On the other hand, total reaction cross sections given by previous optical-model analyses[32,33,37] generally disagree with the measured values.

The present σ_R results for the $p + {}^4\mathrm{He}$ interaction agree with those obtained from a phase-shift analysis[36] in the energy range 20 to 40 MeV and have been used[21] as constraints on the phase shifts in an extension of the analysis to higher energies. The present σ_R results for the $p + {}^3\mathrm{He}$ interaction should prove to be useful input to either phase-shift analyses or resonating-group calculations for that system.

Finally, the present values of σ_R for the $p + {}^4\mathrm{He}$ system were found to be larger than those which had resulted from the inclusion of a phenomenological imaginary potential in a previous[42] resonating group study of that system. New resonating-group calculations were carried out using an imaginary potential whose form is more similar to that used for other systems.[1,39,41] Fits to the elastic data were obtained which are nearly as good as those of Ref. 42 and which generate σ_R values in agreement with the present work. The most significant differences between the present

calculated phase shifts and those from the phase-shift analysis[36] are found in comparisons of the amount of d-wave splitting of the real parts of the phases and in the amount of absorption present in the p waves relative to the d waves.

ACKNOWLEDGMENTS

For valuable help with the experimental apparatus and with data collection we thank N. E. Davison, S. A. Elbakr, J. L. Horton, M. S. de-Jong, J. Rae, and M. Wright; and for aid in computer programming we express gratitude to R. Herzog and P. O'Conner. Discussions with Y. C. Tang and D. R. Thompson about the resonating-group method are gratefully acknowledged. B. Batten and the University of Manitoba mechanical shop are thanked for their help in fabricating portions of the apparatus, and we express our appreciation to the University of Manitoba technical crews for their reliable operation of the cyclotron.

†Work supported in part by the Atomic Energy Control Board of Canada, by the Research Corporation, and by the U. S. Energy Research and Development Administration.

[1]J. A. Koepke, R. E. Brown, Y. C. Tang, and D. R. Thompson, Phys. Rev. C 9, 823 (1974), and references therein.

[2]J. A. Koepke and R. E. Brown, Bull. Am. Phys. Soc. 18, 1382 (1973); John H. Williams Laboratory of Nuclear Physics Annual Report, 1973 (unpublished), p. 32.

[3]P. M. Hegland and R. E. Brown, Bull. Am. Phys. Soc. 18, 1381 (1973); John H. Williams Laboratory of Nuclear Physics Annual Report, 1974 (unpublished), p. 1.

[4]C. H. Poppe, R. E. Brown, P. M. Hegland, and J. A. Koepke, Bull. Am. Phys. Soc. 20, 578 (1975).

[5]T. J. Gooding, Nucl. Phys. 12, 241 (1959).

[6]J. F. Dicello, G. J. Igo, and M. L. Roush, Phys. Rev. 157, 1001 (1967).

[7]J. F. Dicello and G. Igo, Phys. Rev. C 2, 488 (1970).

[8]J. J. H. Menet, E. E. Gross, J. J. Malanify, and A. Zucker, Phys. Rev. C 4, 1114 (1971).

[9]W. F. McGill, R. F. Carlson, T. H. Short, J. M. Cameron, J. R. Richardson, I. Šlaus, W. T. H. van Oers, J. W. Verba, D. J. Margaziotis, and P. Doherty, Phys. Rev. C 10, 2237 (1974).

[10]R. F. Carlson, W. F. McGill, T. H. Short, J. M. Cameron, J. R. Richardson, W. T. H. van Oers, J. W. Verba, P. Doherty, and D. J. Margaziotis, Nucl. Instrum. Methods 123, 509 (1975).

[11]A. M. Sourkes, N. E. Davison, S. A. Elbakr, J. L. Horton, A. Houdayer, W. T. H. van Oers, and R. F. Carlson, Phys. Lett. 51B, 232 (1974).

[12]Suggested by H. Bichsel.

[13]H. Bichsel and C. Tschalaer, Nucl. Data A3, 343 (1967).

[14]The measured cell lengths are accurate to better than ±0.1 mm and include the contributions from the bulging under pressure of the entrance and exit foils.

[15]The ^{4}He mass densities were obtained from R. D. McCarty, U. S. National Bureau of Standards Technical Note No. 631, 1972 (unpublished), and the ^{3}He mass densities were scaled down from those of ^{4}He by the isotopic mass ratio.

[16]C. C. Kim, S. M. Bunch, D. W. Devins, and H. H. Forster, Nucl. Phys. 58, 32 (1964); S. A. Harbison, R. J. Griffiths, N. M. Stewart, A. R. Johnston, and G. T. A. Squier, *ibid.* A150, 570 (1970); J. R. Morales, Ph.D. thesis, University of California, Davis, 1970 (unpublished); R. L. Hutson, N. Jarmie, J. L. Detch, Jr., and J. H. Jett, Phys. Rev. C 4, 17 (1971); J. R. Morales, T. A. Cahill, D. J. Shadoan, and H. Willmes, *ibid.* 11, 1905 (1975).

[17]S. Hayakawa, N. Horikawa, R. Kajikawa, K. Kikuchi, H. Kobayakawa, K. Matsuda, S. Nagata, and Y. Sumi, J. Phys. Soc. Jpn. 19, 2004 (1964).

[18]M. K. Brussel and J. H. Williams, Phys. Rev. 106, 286 (1957); S. N. Bunker, J. M. Cameron, M. B. Epstein, G. Paić, J. R. Richardson, J. G. Rogers, P. Tomaš, and J. W. Verba, Nucl. Phys. A133, 537 (1969).

[19]S. M. Bunch, H. H. Forster, and C. C. Kim, Nucl. Phys. 53, 241 (1964).

[20]K. W. Brockman, Jr., Phys. Rev. 102, 391 (1956); J. Sanada, J. Phys. Soc. Jpn. 14, 1463 (1959); B. W. Davies, M. K. Craddock, R. C. Hanna, Z. J. Moroz, and L. P. Robertson, Nucl. Phys. A97, 241 (1967); P. Darriulat, D. Garreta, A. Tarrats, and J. Testoni, *ibid.* A108, 316 (1968); P. W. Allison and R. Smythe, *ibid.* A121, 97 (1968); D. J. Plummer, K. Ramavataram, T. A. Hodges, D. G. Montague, A. Zucker, and N. K. Ganguly, *ibid.* A174, 193 (1971); A. D. Bacher, G. R. Plattner, H. E. Conzett, D. J. Clark, H. Grunder, and W. F. Tivol, Phys. Rev. C 5, 1147 (1972).

[21]A. D. Bacher, S. A. Elbakr, A. Houdayer, A. M. Sourkes, and W. T. H. van Oers (unpublished).

[22]R. J. Griffiths and S. A. Harbison, Ap. J. 158, 711 (1969).

[23]S. A. Harbison, R. J. Griffiths, F. G. Kingston, A. R. Johnston, and G. T. A. Squier, Nucl. Phys. A130, 513 (1969); C. C. Chang, E. Bar-Avraham, H. H. Forster, C. C. Kim, P. Tomaš, and J. W. Verba, *ibid.* A136, 337 (1969); L. E. Williams, C. J. Batty, B. E. Bonner, C. Tschalär, H. C. Benöhr, and A. S. Clough, Phys. Rev. Lett. 23, 1181 (1969); A. D. Bacher, F. G. Resmini, R. J. Slobodrian, R. de Swiniarski, H. Meiner, and W. F. Tivol, Phys. Lett. 29B, 573 (1969).

[24]S. A. Harbison, R. J. Griffiths, N. M. Stewart, A. R. Johnston, and G. T. A. Squier, Nucl. Phys. A152, 503 (1970).

[25]J. L. Yarnell, R. H. Lovberg, and W. R. Stratton, Phys. Rev. 90, 292 (1953).

[26]D. J. Cairns, T. C. Griffith, G. J. Lush, A. J. Metheringham, and R. H. Thomas, Nucl. Phys. 60, 369 (1964).

[27]J. C. Allred, Phys. Rev. 84, 695 (1951); A. F. Wickersham, Jr., *ibid.* 107, 1050 (1957).

[28]J. G. Rogers, J. M. Cameron, M. B. Epstein, G. Paić,

P. Tomaš, J. R. Richardson, J. W. Verba, and P. Doherty, Nucl. Phys. A136, 433 (1969).
[29]L. H. Johnston, D. H. Service, and D. A. Swenson, IRE Trans. Nucl. Sci. NS-5, 95 (1958); D. F. Measday and C. Richard-Serre, Nucl. Instrum. Methods 76, 45 (1969).
[30]J. D. Seagrave, J. C. Hopkins, D. R. Dixon, P. W. Keaton, Jr., E. C. Kerr, A. Niiler, R. H. Sherman, and R. K. Walter, Ann. Phys. (N.Y.) 74, 250 (1972).
[31]If we assume that the two "charge-exchange" reactions ^{3}He(p, n)3p and ^{3}H(p, n)^{3}He have roughly similar angular distributions, then the approximate symmetry about 90° of the former reaction follows from the trend toward symmetry with increasing energy observed for the latter reaction [W. E. Wilson, R. L. Walter, and D. B. Fossan, Nuc. Phys. 27, 421 (1961)].
[32]B. S. Podmore and H. S. Sherif, in *Few Body Problems in Nuclear and Particle Physics*, edited by R. J. Slobodrian, B. Cujec, and K. Ramavataram (University of Laval Presses, Quebec, 1975), p. 517, and private communication.
[33]L. G. Votta, P. G. Roos, N. S. Chant, and R. Woody, III, Phys. Rev. C 10, 520 (1974).
[34]T. W. Bonner, J. P. Conner, and A. B. Lillie, Phys. Rev. 88, 473 (1952); A. P. Kliucharev, B. N. Esel'son, and A. K. Val'ter, Dokl. Akad. Nauk. SSSR 109, 737 (1956) [Sov. Phys.–Dokl. 1, 475 (1956)]; L. Stewart, J. E. Brolley, Jr., and L. Rosen, Phys. Rev. 119, 1649 (1960); T. R. King and R. Smythe, Nucl. Phys. A183, 657 (1972).
[35]F. Ajzenberg-Selove and T. Lauritsen, Nucl. Phys. A227, 1 (1974).
[36]G. R. Plattner, A. D. Bacher, and H. E. Conzett, Phys. Rev. C 5, 1158 (1972).
[37]G. E. Thompson, M. B. Epstein, and T. Sawada, Nucl. Phys. A142, 571 (1970).
[38]K. Wildermuth and W. McClure, in *Springer Tracts in Modern Physics*, edited by G. Höhler (Springer-Verlag, Berlin, 1966), Vol. 41.
[39]R. E. Brown and Y. C. Tang, Nucl. Phys. A170, 225 (1971).
[40]P. Darriulat, G. Igo, H. G. Pugh, and H. D. Holmgren, Phys. Rev. 137, B315 (1965); A. D. Bacher, F. G. Resmini, H. E. Conzett, R. de Swiniarski, H. Meiner, and J. Ernst, Phys. Rev. Lett. 29, 1331 (1972).
[41]Y. C. Tang and R. E. Brown, Phys. Rev. C 4, 1979 (1971); D. R. Thompson, Y. C. Tang, J. A. Koepke, and R. E. Brown, Nucl. Phys. A201, 301 (1973); F. S. Chwieroth, R. E. Brown, Y. C. Tang, and D. R. Thompson, Phys. Rev. C 8, 938 (1973); R. E. Brown, F. S. Chwieroth, Y. C. Tang, and D. R. Thompson, Nucl. Phys. A230, 189 (1974).
[42]D. R. Thompson, Y. C. Tang, and R. E. Brown, Phys. Rev. C 5, 1939 (1972).
[43]I. Reichstein, D. R. Thompson, and Y. C. Tang, Phys. Rev. C 3, 2139 (1971).
[44]M. LeMere, R. E. Brown, Y. C. Tang, and D. R. Thompson, Phys. Rev. C 12, 1140 (1975).
[45]M. K. Craddock, R. C. Hanna, L. P. Robertson, and B. W. Davies, Phys. Lett. 5, 335 (1963).
[46]T. C. Griffith, D. C. Imrie, G. J. Lush, and L. A. Robbins, Phys. Rev. 146, 626 (1966).
[47]E. T. Boschitz, M. Chabre, H. E. Conzett, E. Shield, and R. J. Slobodrian, in *Proceedings of the Second International Symposium on Polarization Phenomena of Nucleons, Karlsruhe, Germany, 1965* (Birkhäuser, Basel, Switzerland, 1966), p. 328.
[48]In Sec. V, Fig. 4, and Table III all energies E refer to the c.m. system; elsewhere the energies E_p refer to the proton energy in the lab system.